MEASUREMENT GENERATION PROCESS FOR PODIUM, A PULSAR NAVIGATION UNIT FOR SCIENCE MISSIONS

Víctor Gómez Ruiz[a], Francesco Cacciatore[b], Gonzalo Taubmann[c], Jacinto Muñoz[d], Pablo Hermosín[e], Marcello Sciarra[f], Martiño Saco[g], Nanda Rea[h], Margarita Hernanz[i], Emilie Parent[j], J. Vandersteen[k]

[a] *SENER Aeroespacial, victor.ruiz@aeroespacial.sener*
[b] *SENER Aeroespacial, francesco.cacciatore@aeroespacial.sener*
[c] *SENER Aeroespacial , gonzalo.taubmann@aeroespacial.sener*
[d] *SENER Aeroespacial, jacinto.msanchez@aeroespacial.sener*
[e] *Deimos Space SLU, pablo.hermosin@deimos-space.com*
[f] *Deimos Space SLU, marcello.sciarra@deimos-space.com*
[g] *Deimos Space SLU, martino.saco@deimos-space.com*
[h] *Institut d'Estudis Espacials de Catalunya (IEEC) - Consejo Superior de Investigaciones Científicas (CSIC), rea@ice.csic.es*
[i] *Institut d'Estudis Espacials de Catalunya (IEEC) - Consejo Superior de Investigaciones Científicas (CSIC), hernanz@ice.csic.es*
[j] *Institut d'Estudis Espacials de Catalunya (IEEC) - Consejo Superior de Investigaciones Científicas (CSIC), parent@ice.csic.es*
[k] *ESA- ESTEC GNC, AOCS and Pointing division, jeroen.vandersteen@esa.int*

ABSTRACT

PODIUM is a compact spacecraft navigation unit, designed to provide interplanetary missions with autonomous position and velocity estimations. The unit will make use of Pulsar X-ray observations to measure the distance and distance rate from the host spacecraft to the Solar System Barycenter. Such measurements will then be used by the onboard orbit determination function to estimate the complete orbital elements of the spacecraft. The design aims at 6 kg of mass and 20 W of power, in a volume of 150 mm by 240 mm by 600 mm. PODIUM is designed to minimize the impact on the mission operational and accommodation constraints and will enable higher autonomy and lower cost for interplanetary missions. The architecture is based on a grazing incidence X-ray telescope with focal distance limited to 50 cm. The effective area shall be in the range 25 to 50 cm2 for photon energies in the range 0.2-10 keV, requiring nesting of several mirrors in the Wolter-1 geometry. The FOV size will determine the aperture of the optics and be related to the maximum number of nested mirrors to accommodate. The target FOV is 0.25 deg. The expected position accuracy is in the order of 10 km.

1 INTRODUCTION

Autonomous celestial-based navigation is a great alternative to complementing existing orbit determination systems and for the development of future navigation techniques that allow reducing the dependency from Earth. This would help not only to increase the state knowledge and autonomy

of the spacecraft (S/C) in deep space, but also to increase the autonomy level in critical maneuvers and tasks that require a precise orbit determination solution.
The concept of using pulsars for spacecraft navigation has been in development since the 1960's. Among the different electromagnetic bands, the required hardware to detect pulsars in the radio and optical bands would be extremely large to be feasible for flying in space. On the other hand, using X-ray observations, a larger signal to noise ratio (SNR) can be achieved for pulsars using much smaller and lighter equipment.
Different algorithms and methods have been explored in order to include the pulsar observations in the orbit determination process. A key step in X-ray Navigation (XNAV) is the estimation of the pulse phase, using initial position estimate of the S/C and various ephemeris parameters.
The effect of ephemerides errors, satellite clock-errors, and the movement of the spacecraft during the filtering process can degrade the orbit determination solution accuracy. To eliminate the effect of the S/C motion, the phase estimation can be coupled with Doppler frequency. Notice that in order to obtain a sufficiently precise (low-noise) measurement, a sufficient number of photons shall be collected, meaning that the duration and planning of the observation campaign will play a relevant role.
If the number of observations is sufficient, at least four, pulsar navigation can also be used to correct the on-board clock to meet the clock requirements for tracking communication signals. Using pulsar time of arrival and an internal model of the clock, a filtering process can provide the values of the different coefficients of the clock model using the offset between the estimated clock error and the computed clock error as measurements.
The objective of this study is to design and evaluate the performance of an autonomous XNAV unit with a 60x15x24 cm3, 6 kg and 20 W limit, able to be integrated in a wide range of satellites.
The design must be assessed in two operational cases: a typical L2 observatory orbit, and planetary flyby conditions.
The initial accuracy requirements are 10 km position knowledge error with 99% probability at 90% confidence level, at any time during L2 mission nominal science phase or 6 hours before a planetary flyby pericenter.
This paper is focused on the unit measurement generation, further information on the design of the unit can be found in [1].

2 HIGH LEVEL CONCEPT

PODIUM is based on a small telescope with an X-ray detector placed at its focal point. The photons incoming from the pulsar are read at the detector and the timestamps assigned are used by the on-board computer (OBC) to regenerate the signal. This is done over several hours of observation, where the photons are time-folded into a single period until sufficient signal to noise ratio is achieved.
Once a clear signal is obtained, it is compared to the reference signal preloaded on the OBC at the observation time. The time shift between these two signals, along with an estimation of the current position of the spacecraft with sufficient accuracy, allows the generation of a ranging measurement that is then used to improve the estimation of the state of the S/C.
With the objective of designing a small unit with tight Size, Weight and Power (SWaP) constraints, and considering similar instruments, the effective area of the telescope has been designed to be approximately 50 cm2. For the same reason, the unit has no gimbaling capabilities; the host spacecraft must be in charge of the pointing maneuvers. In the case some parameters need to be updated from ground on the OBC, all communications will be carried with the host spacecraft and the information will be passed to the unit through a communications link.
A simulator has been developed to assess the performance of the system. The photon sequence that

would arrive to the telescope is first simulated taking into account the characteristics of the source Pulsar and those of the unit (mainly the effective area and the selected clock and detector errors). Then, a differentiated onboard algorithm, which does not share variables with the photon sequence algorithm and only uses the timestamps as an input, reconstructs the signal and calculates the phase shift and, finally, the distance between the spacecraft and the reference position (usually the Solar System Barycenter (SSB)) in the direction of the pulsar. Finally, a separate algorithm performs the orbit determination using the system measurements.

3 PHYSICAL DESIGN

This section is devoted to the presentation of the optical, mechanical and thermal design for the PODIUM telescope. The main requirement driving the configuration is the need of fitting the target envelope of 600 x 150 x 240 mm^3 and the maximization of the effective area to maximize the accuracy of the measurement over a fixed acquisition time.

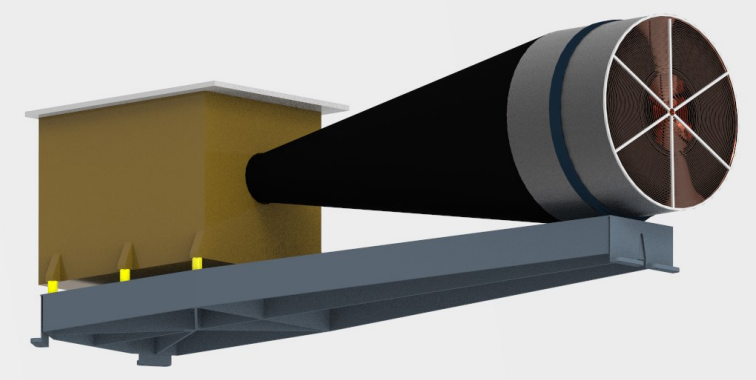

Figure 1. PODIUM instrument concept

3.1 Field of View Sizing and Telescope Configuration

The AOCS accuracies for a host system using PODIUM are prescribed as Absolute Pointing Error (APE) 0.1 deg and Relative Pointing Error (RPE) 0.05 over 1000s, with 99% probability and 90% confidence interval.

This requirement allows a preliminary sizing of the FOV of the detector. The FOV, in fact, shall be large enough to ensure that the targeted pulsar is within the actual FOV considering AOCS pointing APE and RPE, guaranteeing that no photons are lost due to mis-pointing.

In line with this approach, the FOV size (obtained from the optics/collimator and detector combination) was initially proposed in the interval between 0.25 deg and 0.5 deg maximum.

A wider FOV size will imply increasing the area exposed to background noise; this will reduce the SNR of the reconstructed pulsar pulse, implying that longer exposure times might be required to achieve sufficient accuracy, especially in case of faint sources.

The baseline design for PODIUM's telescope is based on Type Walter I design, in which mirrors are composed by a set of nested mirrors in concentric fashion.

The telescope FOV size drives the aperture of the optics and be related to the maximum number of nested mirrors to accommodate. The current target FOV is 0.25 deg aperture.

Typically, combinations of parabolic and hyperboloidal mirrors are used to achieve reflection of collimated rays to a specific focus.

For PODIUM, the main function of the optical and detection assembly is to collect and time pulsar photons, with a baseline design that does not require imaging capability (the selected detector is a

single-pixel Silicon Drift Detector (SDD) with 9.44 mm diameter, see [2]). Therefore, it is not necessary to focus the light to preserve the incoming light direction. Not needing focusing it is possible to substitute the parabolic and hyperboloidal surfaces for conical surfaces. Conical mirrors are easier to manufacture and potentially allow the inclusion of more than two mirror stages in series to reduce the grazing angle at each mirror. Nevertheless, only two consecutive cones per shell are required for PODIUM.
The mirrors are encapsulated in an aluminium cylinder with external diameter 150 mm.
Three design/optimization iterations were carried out for the telescope optical design, resulting in a total of 37 shells distributed in 16 shells with 2 Conical Mirrors in series and 21 shells with a unique Conical Mirror.

3.2 Pulsar Energy Range and Evaluation of the Effective Area

PODIUM is initially designed to detect pulsars in the range of energy between 0.5 keV to 10.0 keV. It should be noticed that the larger is the photons' energy, the smaller shall be the grazing angle on the telescope mirrors to have an efficient reflectivity, leading to a more complex telescope design with a large number of shells and lower overall efficiency.
Fortunately, further analysis of the most feasible pulsars sources allowed to establish that the predominant number of pulsars are in a lower range between 0.5 keV to 2.0 keV. In this range, the grazing angle is not so critical, and a simpler mirror system can be designed.
Each pulsar source has different distribution of energy, and this distribution has been considered by weighting the reflectivity for a given energy with the probability to have a pulsar with this specific range of energy.
The result is a unique equivalent effective energy for each of the selected sources. A reference effective area of approximately 60 cm2 is considered for all selected pulsars.

3.3 Thermo-Mechanical Design

The thermo-mechanical design is driven by the main components, namely the Telescope, the Detector with the Amplifier, and the Electronics.
A preliminary Finite Element Model (FEM) analysis has been carried out to assess the structural response of the design, and to assess its thermo-mechanical behaviour. The FEM analysis has been used to iterate the design and ensure that the first natural frequency of the instrument is above 60Hz.
The mass budget of PODIUM obtained from the FEM model totals approximately 6 kg.
The thermal design focus is to ensure the dissipation of heat of the Electronics and Focal Plane to keep the temperature inside the operational and survival ranges, depending on the functional mode.
The electronics is the power dissipating element, with a maximum power of 12 W.
A thermal analysis was performed, based on the FEM model used for eigen-frequencies determination. The thermal characteristics of the materials have been defined as well as conductivity characteristics of the thermal washers. The FEM model evaluates the temperature distribution for a steady-state case, thus providing the displacement of critical points.
Results show a Line of Sight (LoS) variation of 48 arcsec and a displacement of detector of 600 µm. The deviation of the LoS of 48 arcsec is not critical because it is inside the FOV of the instrument and is much smaller than the pointing accuracy expected for the AOCS system Avionic Design.

3.3.1 Electronic Design

The architecture of PODIUM electronics has been selected by considering the mission requirements/constraints of timing and processing performances, low power consumption, very compact mechanical configuration due to reduced allocated volume, and a good degree of autonomy for fault management.
To achieve these design goals, the PODIUM electronics design must take advantage of the use of complex System-On-Chip (SoC) devices and large Field Programmable Gate Arrays (FPGAs),

allowing to integrate communication, process, and control functionalities in a small volume.

3.3.2 Detector

In order to achieve the high timing accuracy required for PODIUM (better than 1 μs), Silicon Drift Detectors are assumed. The combination of a single-pixel ultrafast SDD detector with the grazing incidence X-ray optics focusing system provides the required effective area.
The FAST SDD® [2] represents Amptek's highest performance silicon drift detector, capable of count rates over 1,000,000 counts per second (CPS) while maintaining excellent resolution, and is chosen as a baseline for the design of the unit..

4 MEASUREMENTS MODEL

A measurement model has been implemented to include pulsar-based measurements. For each observed pulsar, the measurement model provides the range between S/C and SSB projected in the direction of the pulsar by exploiting equation 1:

$$c \cdot (t_{SSB} - t_{S/C}) = f(r_{S/C}, \check{n}, D_{PULSAR}, V_{PULSAR}) \quad (1)$$

According to which the delta elapsed time that takes the light to reach the SSB and the spacecraft is a function of the spacecraft position and the pulsar direction. Additional parameters D_{PULSAR} and V_{PULSAR} are functions of the pulsar intrinsic properties which can be neglected in a first approximation. Therefore, navigation corrects the S/C position along the radial direction observed from the pulsar. Using several sources in the navigation campaign considerably improves the knowledge along all directions.

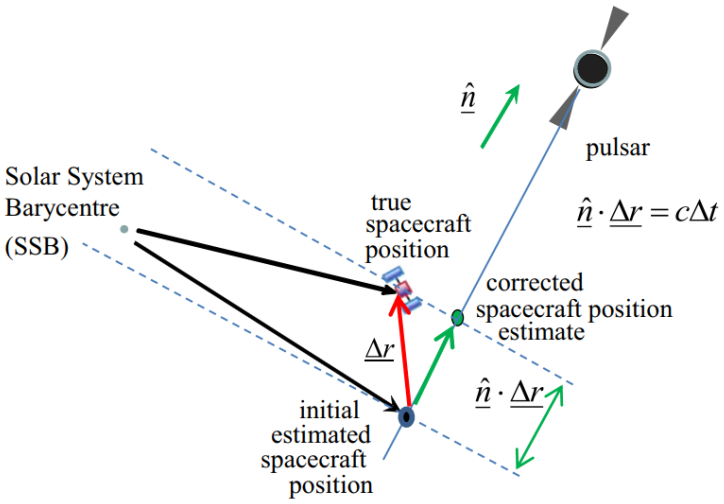

Figure 2. Pulsar-based range measurement representation

According to the presented model, the implemented equivalent pulsar measurement model performs the following steps:

- Retrieves the current spacecraft state
- Retrieves the ephemerides of the Solar System Barycenter (SSB) and the spacecraft state relative to the SSB.
- Computes the unit pulsar direction and projects the state relative to the SSB in the pulsar direction.
- Perturbs the range measurement according to the propagation world.

- Adds clock error contribution.
- Outputs the estimated measurement.

The clock is modelled according to equation 2:

$$clock\_error = b + q1\sqrt{\Delta T} + q2\sqrt{\frac{\Delta T^3}{3}} \quad (2)$$

Where b is the clock bias and $q1$, $q2$ are the coefficients that describe the time evolution of the error, and their values can be found in the datasheet of the corresponding clock.

5 MEASUREMENTS SIMULATOR

The PODIUM activity includes the development of preliminary measurement algorithm and the simulation of the unit performance. Such simulation is achieved via two simulators used in sequence: the first simulator is used to simulate the pulsar pulse reception and the ranging measurements generation, while the second is an Orbit Determination simulator using a performance model of the PODIUM pulsar measurements, as explained in [1].
The pulsar measurement simulator, described in this section, is in turn divided into two parts: the photon sequence generation and the pulse processing and measurement generation. The purpose of this section is to present the preliminary breakdown of operations and their implementation.

5.1 Photon Sequence Generation

The time at which the photons hit the sensor at the spacecraft must be simulated to have a realistic scenario for the rest of the computationsto be performed over this data.
To do this, the following steps are done:

1) Retrieve pulsar data from an observatory: For this simulation, timing files for the J0030+0451 pulsar have been retrieved from the pulsar catalogue [see PULSAR SKY CATALOGUE]. These files give you the light curve in terms of counts per phase bin, illustrated with blue circles in Figure 3.
2) Move phase of data from the reference time to the observation time.
3) Perform a multiple gaussian fitting to this data: In the case of the example, 2 gaussian distributions have been fit to the data using the least squares method. The result is illustrated in Figure 3.
4) Generate signal photon hits: timestamps are generated from the Gaussian distributions using a Non-Homogeneous Poisson Process (NHPP) at the rates specified for the signal from the pulsar catalogue for the input effective area. These photons are generated at the same reference frame as the original data, usually the Solar System Barycenter, at the observation time.
5) Generate noise photon hits: timestamps are generated using a Homogeneous Poisson Process (HPP) at the rates specified for the noise from the pulsar catalogue for the input effective area. The sum of the signal and noise photons is received by the telescope.
6) Transfer photons to the spacecraft: the timestamps are transferred from the SSB to the position of the spacecraft using the light-time between the two points [3]. The timestamps generated in 0.5 hours of observation with an effective area of 60 cm^2 are depicted in Figure 4.

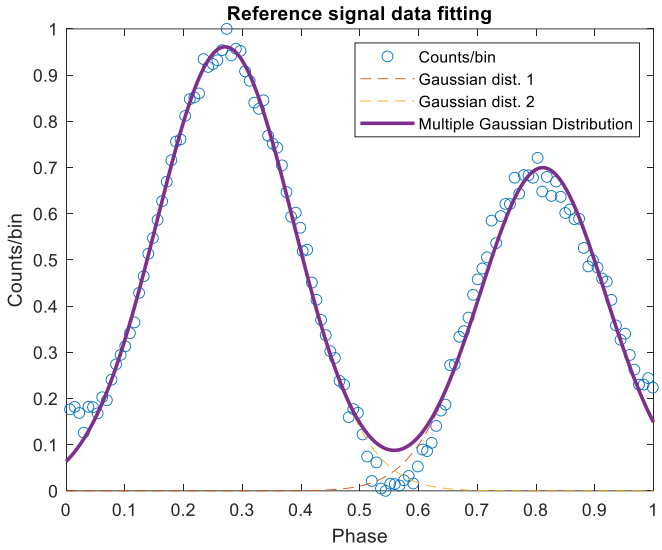

Figure 3. Reference data multiple Gaussian fitting

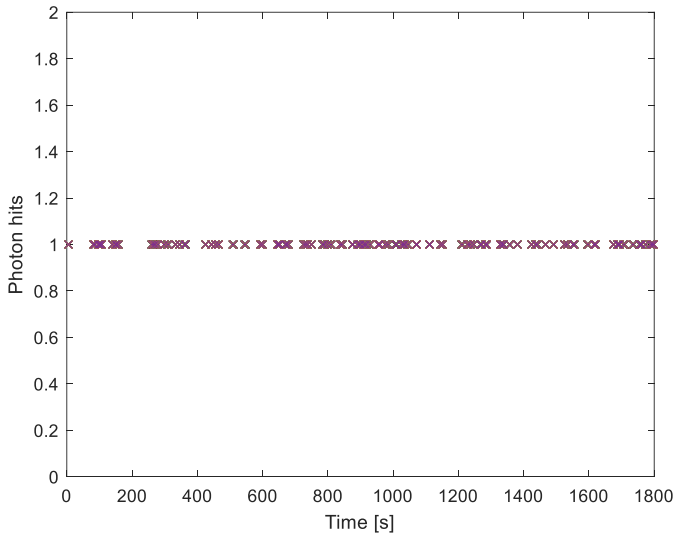

Figure 4. Timestamps of photons at the telescope for 0.5 hours of observation. Aeff = 60 cm2. Pulsar: J0030+0451

7) Add clock and detector errors:

- Detector errors: two factors are considered when adding the detector errors. The dead-time and the delay. The delay is simply added to the timestamps. The dead-time is implemented by checking the difference between consecutive timestamps. If a photon is received within the dead-time span from a previous hit, it is discarded.
- Clock errors: a model of the clock is simulated using Simulink and the characteristics of the selected clock. The error extracted from this simulation is added to the timestamps. A more detailed overview of the clock is presented in section Clock Model.

5.1.1 Clock Model

The clock model simulates the error created by the clock. It is a timing error that will directly affect the precision of the measurements at a rate of 300 km/s. Therefore, it is of great importance selecting a clock with negligible errors over the time span of an observation. This error is formed by three differentiated components:

- **Clock biases:** constant errors over the time of an observation. Affect all timestamps in the same way and result in a distance measurement bias. Can be corrected from ground.
- **Clock drifts:** not constant during the time of an observation. It is caused by instabilities of the clock and result in a deformation of the profile.
- **Clock noise:** high frequency error that affects every photon in a different way and results in a noisy signal.

The long-term stability effects can be corrected from the navigation algorithm by observing at least four pulsars, but with a limited accuracy, as this number of observations will take longer time spans than the stability of the long-term effects.
The clock model used accounts for these effects and is driven by equations 3 and 4:

$$\dot{x}(t) = w(t) + \xi_1(t) \tag{3}$$

$$\dot{w}(t) = \xi_2(t) \tag{4}$$

where $\xi_1(t)$ is the White Frequency Noise (WFN) and $\xi_2(t)$ is the Random Walk Frequency Noise (RWFN). $q1$ is the variance of the WFN and $q2$ the variance of the RWFN, and are extracted from the datasheet of the clocks [4]. The model is implemented in Simulink as in Figure 5:

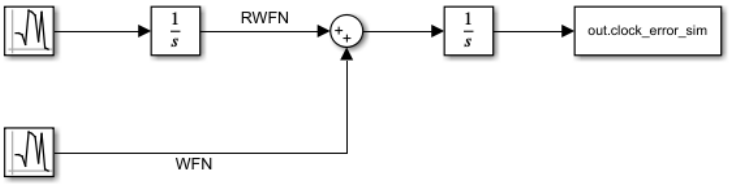

Figure 5. Clock Simulink model

The output of the simulation, depicted in Figure 6, represents the 3σ of the error in seconds (red and orange curves), and the output of the actual simulation (purple), which is used by the simulator to add the error to the timestamps received by the detector.

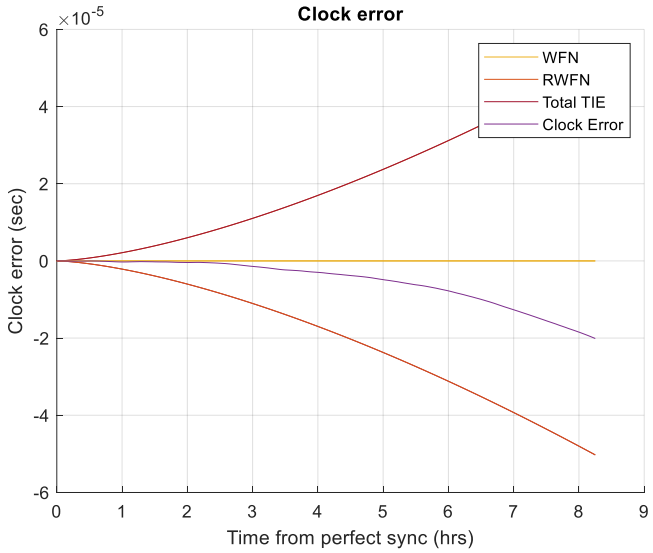

Figure 6. Clock error from simulation (single shot)

5.2 Pulse Processing and Measurement Generation

The steps carried out to simulate the pulse processing to estimate the distance to the SSB are:

1) Time-folding of the timestamps: fold all the timestamps into a single period.

2) Convert Time of Arrivals (TOAs) into Phase of Arrivals (POAs): Convert TOAs to POAs using the expression 5.

$$\phi(t) = \phi_0 + f(t_0)(t - t_0) + \frac{\dot{f}(t_0)}{2}(t - t_0)^2 + \frac{\ddot{f}(t_0)}{6} + (t - t_0)^3 \quad (5)$$

The photons generated for 0.5 hours of observation with an effective area of 60 cm2 are depicted in Figure 7.

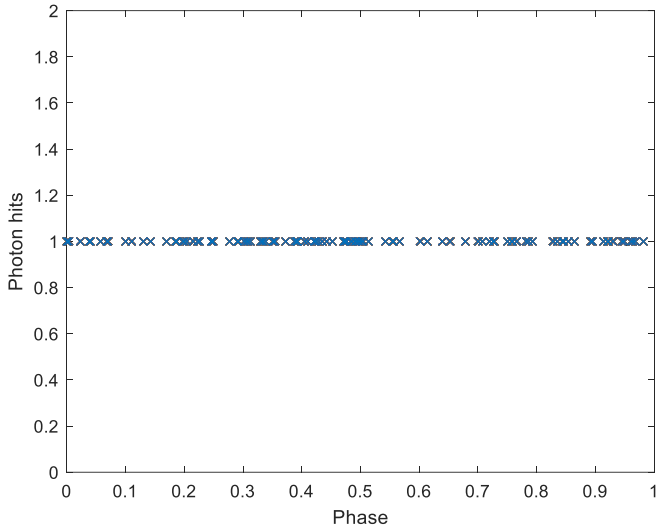

Figure 7. Photon hits for 0.5 hours of observation. Aeff = 60 cm2. Pulsar: J0030+0451

3) Divide counts in phase bins: The previous counts are now divided into phase bins. The size of the bins is defined according to the number of photons received. More photons received mean a clearer signal, allowing smaller bin sizes (more bins) for a more accurate representation of the data. In this simulation, 8 hours of observation with an effective area of 60 cm^2 are simulated. The Counts/bin data can be observed in Figure 8.
4) Fit the signal to the data: Two different methods have been implemented to perform this step. The first consists of performing a multiple Gaussian fitting to the received photons, similar to the first step performed over the reference data. The second method consists of getting the equation of the fitting performed over the reference data, and simply adjusting the phase to the received photons, using the least squares method. It has been found that the second method leads to more accurate results. The outcome of this fitting can be observed in Figure 8.

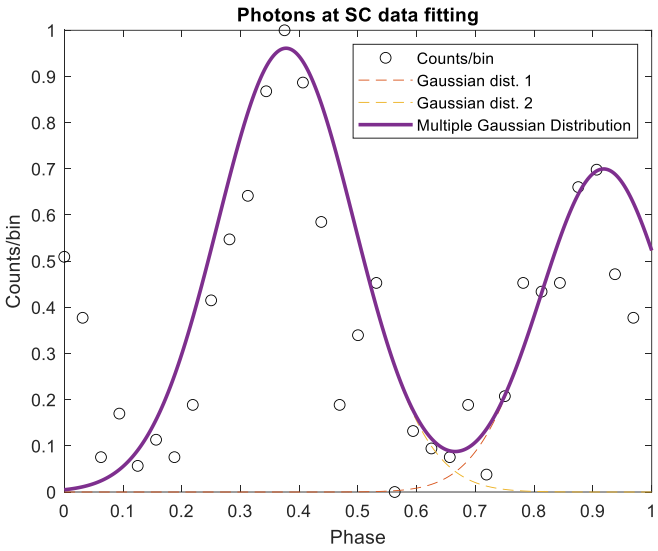

Figure 8. Received data signal fitting. 8 hours observation. Aeff = 60 cm2. Pulsar: J0030+0451

5) Calculate phase shift: The phase shift between the reference signal (moved to the estimated position of the spacecraft) and the signal received by the spacecraft is calculated by comparing the maximums of both signals. The phase shift is illustrated in Figure 9.
6) Calculate the distance: Using an estimate of the distance within half the distance the light travels during a period, and the phase shift, the distance from the spacecraft to the SSB in the pulsar direction is calculated. The results for this example simulation are the following:

Distance from SSB = 1460300 km
Initial knowledge error = -200 km,
Distance estimation error = 7.846 km

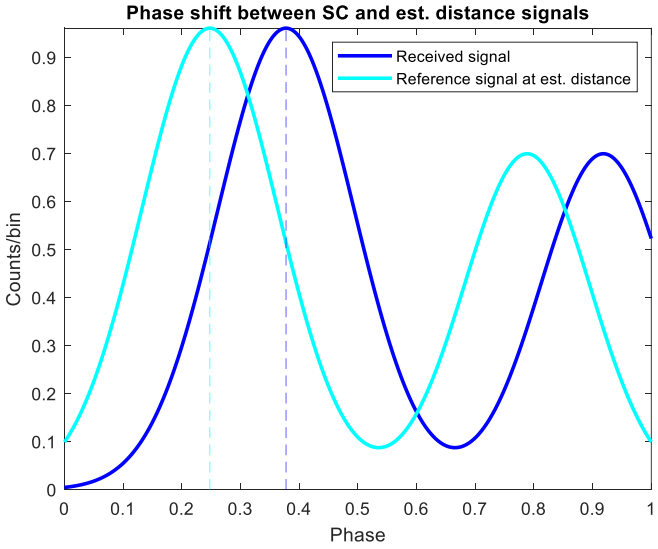

Figure 9. Phase shift between reference signal at estimated position and actual signal at spacecraft

5.3 Data Flow Between Algorithms

The variables needed as input to operate each part of the simulator are presented in Figure 10. The transmission of data between the two main parts of the algorithm is also depicted. It can be seen that

the only inputs needed by the onboard algorithm are the timestamps (generated by the front-end electronics upon photon hits) and the moved reference probability density function (generated when a new pulsar is selected).

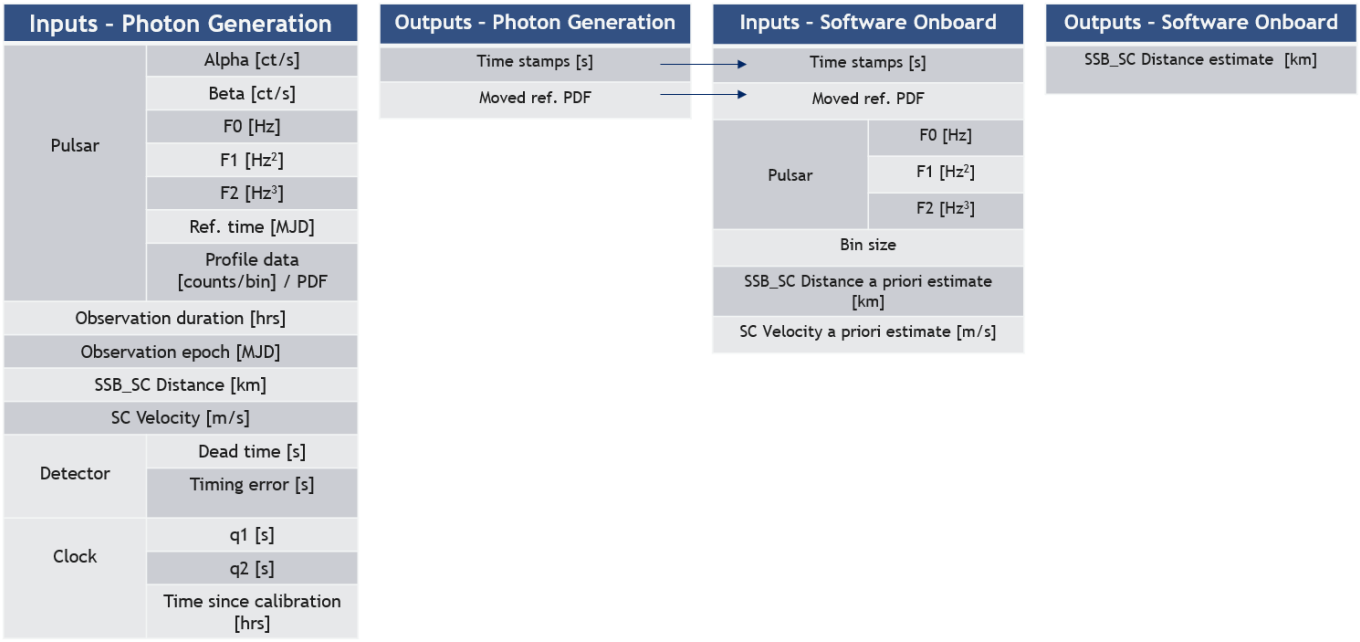

Figure 10. Data flow between algorithms

6 PULSAR SKY CATALOGUE

The main factors that must be considered when selecting targets for an X-ray pulsar navigation system are 1) the timing stability of the pulsar (i.e., the predictability of the pulse phase) and 2) the pulsed flux in the X-ray band, which impacts the precision of the pulse times-of-arrival measurements. The PODIUM pulsar catalogue presented here contains 14 objects spread across the sky that were selected based on their rotational stability and brightness in the soft X-rays. Figure 11 shows their celestial location in Galactic coordinates. Pulsed radio emission is also present in these sources, from which timing parameters have been measured with high precision.

Among the 14 pulsars in the catalogue, 12 of them are nearby millisecond pulsars (MSPs) that have been monitored over the past several years with high-time resolution radio facilities. These observations have been carried out for pulsar timing array experiments such as the European Pulsar Timing Array [5], the North American Nanohertz Observatory for Gravitational Waves [6] and the Parkes Pulsar Timing Array [7]. Together they make up the International Pulsar Timing Array [8] (IPTA), which now includes 65 pulsars. Pulsar Timing Arrays (PTAs) aim to detect a stochastic gravitational wave (GW) background using an array of high-precision MSPs, and their success relies on the stability of the forming the array and the detectability of the disturbances in the pulse TOAs caused by passing GWs. Sources that have been included in the PTA are the absolute cosmic clocks. Their robust ephemerides can accurately predict the pulsar rotational phase for several years following the last timing measurement. All but one of the 12 MSPs in the PODIUM catalogue are PTA sources. The suitability for inclusion of the non-PTA MSP, PSR J1231-1411, is currently being investigated.

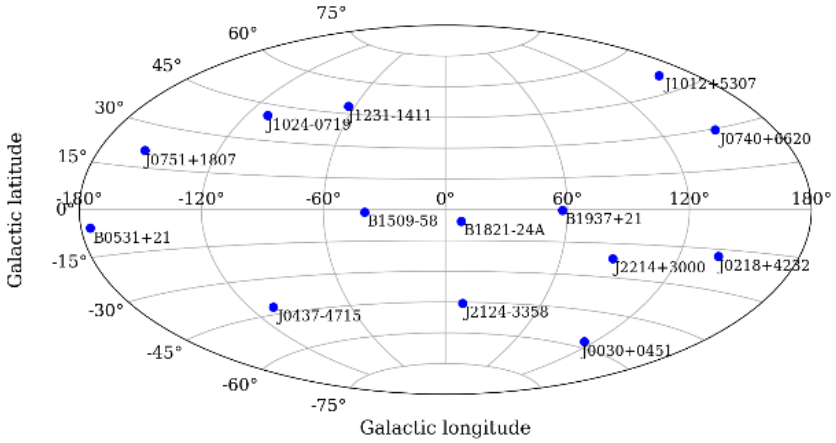

Figure 11. Galactic distribution of the 14 pulsars contained in the PODIUM catalogue

The remaining two pulsars in our catalogue are young and highly energetic pulsars: PSRs B0531+21 (the Crab pulsar) and B1509-58. Their high fluxes across the X-ray band and narrow pulse profiles offer the opportunity to measure high-quality TOAs in very short integrations, making them appealing targets for spacecraft navigation. For example, a statistical precision of a few tens of microseconds can be achieved for pulsations from the Crab from a 5-min observation with an instrument with capabilities similar to that of NICER. A significant drawback however is their noisy rotations, particularly for the Crab, which limits the predictions accuracy of the extrapolated timing model to only a few days.

7 PERFORMANCE ASSESSMENT

7.1 Measurements Performance

To assess the performance of PODIUM when observing different pulsars, a simulation campaign has been performed over all the pulsars in the pulsar catalogue. For each pulsar, 300 simulations have been run for different observation durations and different effective areas, but for Crab, where 100 simulations are enough to accurately represent its response due to its high intensity. The selected clock for the simulations has been the Rakon RK407 and the detector the Amptek FAST SDD. The simulation campaign has been repeated for the following effective areas: 25 cm2, 50 cm2, and 80 cm2.
As a result of each campaign the 3-sigma curve of the confidence in the error for each pulsar is extracted.

The evaluation of the performance of the system for two of the pulsars that give the most accurate results is presented as an example in Figure 12. The curves represent the 3sigma deviation of the data for different integration times and effective areas.

Results (Table 1) show that 6 of the 14 pulsars evaluated are bright enough to provide a significant improvement wrt the initial knowledge error (Crab, B1509-58, J0030+0451, J0437-4715, J2124-3358, J1231-1411) (in green). The rest provide a rate of photons too low to perform good measurements with the effective area of our instrument: the photons received are too scattered for the system to perform a good fitting over them. If the received photons do not represent the original pulse even so slightly, it is not possible to adjust the signal to the received data.

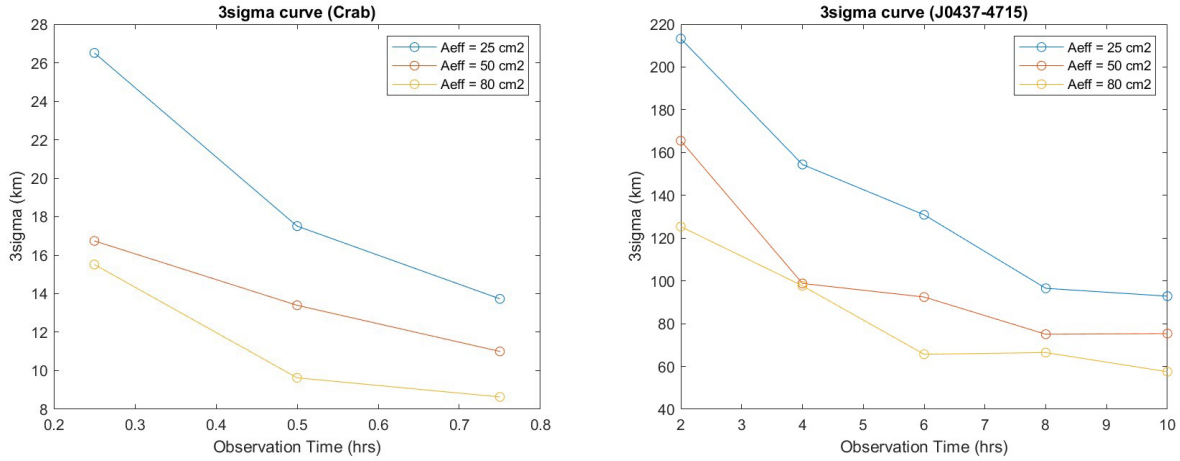

Figure 12. Measurements Performance for Pulsars Crab and J0437-4715

An important aspect of the pulsars is the frequency. The lower it is, the higher the initial knowledge error can be. Certain pulsars with low frequencies (B1509-58, Crab) can be used to narrow the initial knowledge error, so the accuracy of the position can be then improved with measures of higher frequency pulsars.
Frequency also affects the precision of the distance calculation. An error in the phase fitting represents a higher error in the distance in a pulsar with low frequency (a lower frequency means a higher period: an error in the phase means a larger time span if the period is higher. A larger time span of error means a higher distance error).
A special case is the B1509-58 pulsar (in orange in Table 1), which has a very low frequency and allows to reduce the error from 22720 km to around 200 km. Higher precisions are not achieved due to the low frequency of the pulsar.
The intensity of the pulsar determines along the SNR the observation time needed to accurately reconstruct the pulse. The more intensity, the less time needed.
The shape of the pulses also affects the precision of the system. Diffuse peaks (with high deviations) are difficult to reconstruct as the noise scatter the time-tags of the photons. Very sharp peaks (with low deviations) are difficult to detect as a small number of photons are received from the very moment of the peak.
The non-linearity of the error with respect to the observation time can be attributed to the inclusion of the clock error to the simulations, and to the effect of the errors in the fittings to the data.
The clock error increases with time, not allowing the system to reach negligible errors no matter how high the duration of the observation is. For large observation times, the definition of the signal is higher, but phase shifted, therefore increasing the error.

For pulsars with low count rates (such as J1012+5307 or J1024-0719), and for the effective area of our system (around 60 cm2), the measurements quality does not increase with the observation time, as the received photons are too disperse to reconstruct the original signal. For those pulsars to be useful for a system of this characteristics, very long observations with a very stable clock would be needed.

Table 1: Measurements Performance Assessment for all Pulsar Catalogue. Error in km.

	Observation time [hrs] [Effective area cm2]								
Pulsar	0.25			0.5			0.75		
	25	50	80	25	50	80	25	50	80
Crab	26.5	16.7	15.5	17.5	13.3	9.6	13.7	11.0	8.6

	Observation time [hrs] Effective area [cm2]														
Pulsar	2			4			6			8			10		
	25	50	80	25	50	80	25	50	80	25	50	80	25	50	80
B1509-58	755.3	543.2	458.6	583.6	419.8	291.8	486.1	324.2	250.7	392.4	253.7	207.5	345.3	248.9	178.6
B1937+21	321.7	313.6	326.4	301.6	324.5	328.8	323.8	335.1	301.4	316.5	315.5	307.9	313.7	298.7	255.7
B1821-24	590.5	579.0	614.1	603.0	603.6	500.7	583.1	481.5	449.0	587.2	503.5	408.5	592.4	417.2	273.6
J0218+4232	541.8	561.8	576.8	564.7	535.2	537.7	560.6	533.0	534.2	543.7	527.8	527.2	517.2	536.9	528.3
J0030+0451	485.9	349.6	245.2	335.7	200.7	154.4	284.9	170.3	102.5	192.5	81.4	85.0	160.2	72.8	53.0
J1012+5307	604.2	667.4	623.7	609.5	532.7	434.2	628.7	516.5	384.0	550.7	523.9	349.9	539.3	450.6	267.3
J0437-4715	213.2	165.5	125.3	154.4	98.7	97.6	130.8	92.4	65.6	96.5	75.0	66.4	92.8	75.3	57.5
J2124-3358	838.7	638.2	611.6	721.7	489.6	395.3	588.1	469.9	254.3	567.5	315.2	154.3	491.9	325.4	137.2
J2214+3000	642.9	580.0	604.0	639.5	617.2	604.4	584.1	543.3	569.7	582.6	588.8	585.6	562.9	576.4	589.4
J0740+6620	631.1	654.1	649.7	645.8	653.6	645.8	652.8	670.8	642.4	644.7	635.4	631.7	658.0	653.4	632.9
J0751+1807	604.7	578.5	568.5	595.8	524.2	543.6	559.8	537.8	531.0	543.5	539.9	481.6	562.0	517.9	453.0
J1024-0719	795.8	789.4	779.4	743.1	752.3	724.4	744.5	680.7	735.6	731.4	679.8	691.7	781.1	689.6	698.3
J1231-1411	389.8	275.4	217.7	262.8	206.4	173.6	217.3	135.4	112.6	163.2	109.4	81.5	150.5	92.4	73.2

7.2 Orbit Determination Performance

7.2.1 Description of Simulator

An orbit determination (OD) simulator is used to execute the required performance analysis. The pulsars sky catalogue is used to define the pulsars coordinates, while the outputs of the simulation campaign are used to the define the noise level associated to the measurements of each of the pulsars in the catalogue. The OD algorithm is illustrated in [9].

The simulator is designed with the following architecture:

- LOTNAV is used as an OD simulator, which performs Monte-Carlo analysis given the trajectory data, the scheduling of the measurements and the associated noise level.
- A Python orchestrator has been used in order to perform the following tasks:
  - Wrap the call to LOTNAV, allowing to easily set inputs and retrieve outputs.
  - Define the observations scheduling and retrieve the measurement noises associated to the given input acquisition times.
  - Retrieve the outputs of the MC analysis and plot.

7.2.2 Orbit Determination Simulation Campaign Conclusions

The system performance has been tested through the OD simulator under different conditions an L2 observatory scenario and an interplanetary flyby scenario. Some of the relevant conclusions that can be drawn are the following:

- The best achievable performance with the current version of the pulsar catalogue is to keep the position knowledge around 10 km and the velocity knowledge below 1 cm/s, which is considered acceptable for routine operations in the mentioned scenarios.
- The inclusion of, at least, a small number of objects with higher accuracy (achieved thanks to

the high flux of the observed pulsars, Crab for instance) in the positioning is key to keep error levels closer to the 10 km bound.
- The effective area of the telescope does not have a major impact in the 25cm2 to 80cm2 range, relatively to the performance achievable with the current catalogue version. What drives the accuracy based on the results obtained is the pulsars intensity.
- The availability i.e., the scheduling of the measurements, strongly affects the transient phases of the estimation. An important aspect of such scheduling would be to include extensive acquisition campaigns whenever the a-priori knowledge is expected to be very high. This happens, for instance, at the beginning of the simulations and immediately after the flyby.
- The acquisition time has a visible effect on the performance. Shorter acquisitions have lower accuracy but allow for more measurements to be processed, slightly counteracting the performance decrease. Nevertheless, the achievable performance is clearly worse than the baseline case.

A more detailed explanation on the OD process can be found in [1].

8 CONCLUSIONS

The work performed on PODIUM successfully produced a feasible preliminary design for an autonomous interplanetary navigation unit.
PODIUM is based on a Wolter Type I telescope with conic mirrors, with a field of view of 0.25 deg and an effective area of approximately 60 cm^2. A single pixel SDD detector without imaging capabilities is employed. The overall mass of the unit is below 6 kg, with a volume of approximately $600 \times 150 \times 190$ mm. A preliminary measurement generation algorithm has been designed and implemented. The OD performances have been tested with the Pulsar Sky Catalogue produced, and for the L2 orbiter and planetary flyby scenario, with performances in the order of 10 km accuracy when bright pulsars are included in the estimation.
As future activity the development of a breadboard for the pulsar acquisition and measurement generation chain for hardware-in-the-loop demonstration of the functionality could be carried out.
This work has been carried out under ESA contract Contract No. 4000132043/20/NL/CRS/vr.

9 REFERENCES

[1] Cacciatore, Francesco, et al. PODIUM: A Pulsar Navigation Unit for Science Missions. arXiv preprint arXiv:2301.08744, 2023.
[2] FAST SDD® Ultra High Performance Silicon Drift Detector https://www.amptek.com/products/x-ray-detectors/fastsdd-x-ray-detectors-for-xrf-eds/fastsdd-silicon-drift-detector . Retrieved 2022.
[3] Sheikh, Suneel I., et al. "Spacecraft navigation using X-ray pulsars." *Journal of Guidance, Control, and Dynamics* 29.1 (2006): 49-63.
[4] Rakon RK407 Datasheet https://www.rakon.com/products/ocxo-ocso/high-reliability-space-ocxo. Retrieved 2022.
[5] European Pulsar Timing Array http://www.epta.eu.org/. Retrieved 2022.
[6] Nanohertz Observatory for Gravitational Waves http://nanograv.org/. Retrieved 2022.
[7] Parkes Pulsar Timing Array https://www.atnf.csiro.au/research/pulsar/ppta/.Retrieved 2022.
[8] International Pulsar Timing Array http://ipta4gw.org/. Retrieved 2022.
[9] Hermosín, Pablo, et al. "LOTNAV: a low-thrust interplanetary navigation tool." 7th International Conference on Astrodynamics Tools and Techniques (ICATT). 2018.